J Physiol 589.20 (2011) pp 4885–4901

The Journal of Physiology

Age-dependent remodelling of inhibitory synapses onto hippocampal CA1 oriens-lacunosum moleculare interneurons

Charleen Salesse, Christopher Lacharité Mueller, Simon Chamberland and Lisa Topolnik

Axis of Cellular and Molecular Neuroscience, CRULRG, Department of Biochemistry, Microbiology and Bioinformatics, Université Laval, Québec, PQ, Canada

Non-technical summary The main function of the inhibitory synapse is to provide the membrane hyperpolarization and, thereby, to control the level of activity of its target cell. Extensively studied in pyramidal neurons, the properties of inhibitory synapses that target inhibitory interneurons remain largely unknown. We studied the properties of inhibitory synapses formed onto interneurons involved in the hippocampal feedback inhibitory circuit. Our data revealed a significant, age-dependent strengthening of inhibition of interneurons due to the synaptic incorporation of the α5 subunit of the $GABA_A$ receptor. This novel mechanism of age-dependent refinement of local circuit inhibition may have a direct impact on the hippocampal network activity and performance during development.

Abstract Stratum oriens-lacunosum moleculare interneurons (O-LM INs) represent the major element of the hippocampal feedback inhibitory circuit, which provides inhibition to the distal dendritic sites of CA1 pyramidal neurons. Although the intrinsic conductance profile and the properties of glutamatergic transmission to O-LM INs have become a subject of intense investigation, far less is known about the properties of the inhibitory synapses formed onto these cells. Here, we used whole-cell patch-clamp recordings in acute mouse hippocampal slices to study the properties and plasticity of GABAergic inhibitory synapses onto O-LM INs. Surprisingly, we found that the kinetics of inhibitory postsynaptic currents (IPSCs) were slower in mature synapses (P26–40) due to the synaptic incorporation of the α5 subunit of the $GABA_A$ receptor (a5-$GABA_A$R). Moreover, this age-dependent synaptic expression of a5-$GABA_A$Rs was directly associated with the emergence of long-term potentiation at IN inhibitory synapses. Finally, the slower time course of IPSCs observed in O-LM INs of mature animals had a profound effect on IN excitability by significantly delaying its spike firing. Our data suggest that GABAergic synapses onto O-LM INs undergo significant modifications during postnatal maturation. The developmental switch in IPSC properties and plasticity is controlled by the synaptic incorporation of the a5-$GABA_A$R subunit and may represent a potential mechanism for the age-dependent modifications in the inhibitory control of the hippocampal feedback inhibitory circuit.

(Resubmitted 29 June 2011; accepted after revision 2 August 2011; first published online 8 August 2011)
Corresponding author L. Topolnik: Axis of Cellular and Molecular Neuroscience, 2601 Ch. De La Canardière, CRULRG, Québec, PQ, G1J 2G3, Canada. Email: lisa.topolnik@crulrg.ulaval.ca

Abbreviations ACSF, artificial cerebrospinal fluid; $GABA_A$R, $GABA_A$ receptor; CV, coefficient of variation; eIPSC, evoked inhibitory postsynaptic current; ISIs, interneuron-selective INs; LTP, long-term potentiation; O/A, stratum oriens/alveus; O-LM, oriens-lacunosum moleculare; PPR, paired-pulse ratio; sIPSC, spontaneous inhibitory postsynaptic current.

DOI: 10.1113/jphysiol.2011.215244

Introduction

Hippocampal GABAergic interneurons (INs) comprise a diverse population of cells with highly specialized organization and functions. Different subtypes of hippocampal inhibitory INs control spike initiation and synaptic integration by pyramidal neurons and synchronize local network activity, providing a means for functional segregation of neuronal ensembles and proper routing of hippocampal information (Freund & Buzsaki, 1996; Klausberger & Somogyi, 2008). Compared with principal cells, GABAergic INs exhibit specific dendritic and axonal organization, intrinsic biophysical and synaptic properties, network activity, and brain-state-dependent firing behaviour (Freund & Buzsaki, 1996; McBain & Fisahn, 2001; Soltesz, 2006; Klausberger & Somogyi, 2008). Moreover, some classes of hippocampal INs are synaptically interconnected (Ribak 1978; Buhl *et al.* 1995; Sik *et al.* 1995; Acsády *et al.* 1996; Gulyás *et al.* 1996; Cobb *et al.* 1997; Bartos *et al.* 2001; Ali, 2007; Karson *et al.* 2009) and form dynamically interacting inhibitory circuits that are necessary for coordinated network inhibition. However, despite extensive investigation of hippocampal inhibition, the properties and dynamics of inhibitory connections between distinct classes of hippocampal INs remain poorly understood.

To date, several studies of inhibitory synapses onto hippocampal INs have revealed the variability of the kinetics of postsynaptic currents, which is consistent with electrotonic filtering and/or complex molecular organization of the underlying $GABA_A$ receptors ($GABA_A$Rs) (Hájos & Mody, 1997; Bartos *et al.* 2001; Patenaude *et al.* 2001). For instance, the analysis of a total inhibitory drive received by a population of INs in the stratum oriens/alveus (O/A) demonstrated that inhibitory synapses onto these cells are assembled from a combination of various $GABA_A$R subunits (α1–5, β1–3, γ1–3; Patenaude *et al.* 2001). Given the specific co-assembly and cellular and subcellular distribution of different subunits (Fritschy & Mohler, 1995; Nusser *et al.* 1998), inhibitory synapses onto distinct subtypes of O/A INs are likely to exhibit specific biophysical and pharmacological properties. Nevertheless, the cell-type-specific properties of transmission and plasticity at inhibitory synapses onto hippocampal INs remain largely unknown.

Here, we focused on a single population of O/A INs: oriens-lacunosum moleculare (O-LM) cells in the CA1 area of the hippocampus (Lacaille *et al.* 1987; Blasco-Ibáñez & Freund, 1995; Sik *et al.* 1995). These cells play a distinct role in the dialogue of local circuitry by providing feedback inhibition to the distal dendritic sites of pyramidal neurons and, therefore, controlling the perforant path integration (Lacaille *et al.* 1987). This subtype of inhibitory INs, which is easily identifiable morphologically, represents one of the best-studied IN populations of the hippocampus (Maccaferri & Lacaille, 2003). However, while most research to date has focused on the intrinsic conductance profiles and properties of excitatory transmission (including two distinct forms of long-term plasticity; Perez *et al.* 2001; Lamsa *et al.* 2007) in O-LM INs, the properties and dynamics of inhibitory synapses onto these cells have received little attention and were investigated in the present study.

Methods

Slice preparation

All experiments were carried out in accordance with the animal welfare guidelines of the Université Laval. Hippocampal slices were prepared from C57BL/6 (Charles River, St Laurent, PQ, Canada) or Gabra5$^{-/-}$ mice. The Gabra5$^{-/-}$ breeding pairs, originating at Merck (Sharp and Dohme, Harlow, UK) and backcrossed for at least 15 generations onto C57BL/6, were generously provided by Dr I. Mody. Given that most strains achieve a mature stage and are considered as adult animals by P25 (Fox, 2007) as well as the particularities of maturation of the GABAergic system (Luhmann & Prince, 1991; Dunning *et al.* 1999; Yu *et al.* 2006), we increased the animal age used in our experiments to P40. Therefore, according to the mouse developmental stages, two animal age groups were used in these experiments: juvenile (P14–24) and adult (P26–40). Animals were deeply anaesthetized with isoflurane, decapitated and the brain was removed rapidly. Transverse slices (300 μm in thickness) were prepared using a vibratome (Leica VT1000 S; Leica Microsystems, Wetzlar, Germany) in ice-cold (0 to +4°C) 'cutting' solution containing (in mM): 250 sucrose, 2 KCl, 1.25 NaH_2PO_4, 26 $NaHCO_3$, 7 $MgSO_4$, 0.5 $CaCl_2$ and 10 glucose, saturated with 95% O_2 and 5% CO_2, pH 7.4, 320–340 mosmol l^{-1}. Slices were immediately transferred to a heated (35°C), oxygenated 'recovery' solution containing (in mM): 124 NaCl, 2.5 KCl, 1.25 NaH_2PO_4, 26 $NaHCO_3$, 3 $MgSO_4$, 1 $CaCl_2$ and 10 glucose (30 min), after which they were kept at room temperature until use.

Electrophysiology

During experiments, slices were continuously perfused (2 ml min^{-1}) with standard artificial cerebrospinal fluid (ACSF) containing (in mM): 124 NaCl, 2.5 KCl, 1.25 NaH_2PO_4, 26 $NaHCO_3$, 2 $MgSO_4$, 2 $CaCl_2$ and 10 glucose, saturated with 95% O_2 and 5% CO_2, pH 7.4, 295–305 mosmol l^{-1}, at near-physiological temperature (30–33°C). Whole-cell voltage-clamp or current-clamp recordings were obtained from visually identified,

horizontally oriented INs located in the O/A using glass pipettes of 3.5–6 MΩ. For recordings of evoked inhibitory postsynaptic currents (eIPSCs), the pipette solution contained the following (in mM): 130 $KMeSO_3$, 2 $MgCl_2$, 10 disodium phosphocreatine, 10 Hepes, 2 QX-314, 2 ATP-Tris and 0.2 GTP-Tris, plus 0.15–0.2% biocytin, pH 7.25–7.35; 275–285 mosmol l^{-1}. For current-clamp recordings, QX-314 was omitted from the recording solution. For recordings of spontaneous IPSCs (sIPSCs), the pipette solution contained (in mM): 130 $CsMeSO_3$, 2 CsCl, 10 disodium phosphocreatine, 10 Hepes, 2 QX-314, 2 ATP-Tris and 0.2 GTP-Tris, plus 0.15–0.2% biocytin, pH 7.25–7.35; 275–285 mosmol l^{-1}. Series resistance (8.5–23 MΩ) was monitored during all experiments by applying small hyperpolarizing voltage steps (−5 mV), and the recordings were discontinued if the change in series resistance was greater than 15%. Monosynaptic IPSCs were evoked at 0.1 Hz by minimal stimulation of the local hippocampal inhibitory projections using an electrode positioned at the border between the stratum pyramidale and the stratum radiatum in the CA1 area. A stimulation pipette (2–3 MΩ) was filled with ACSF and connected to a constant current isolation unit (A360LA; World Precision Instruments Inc., Sarasota, FL, USA) controlled by a data acquisition board (Digidata 1440; Molecular Devices, Sunnyvale, CA, USA) and Clampex 10.2 software (Molecular Devices). IPSCs were recorded at −40 mV in the presence of the NMDA and AMPA/kainate receptor antagonists DL-AP5 (50 μM; Ascent Scientific, Princeton, NJ, USA) and NBQX (10 μM; Ascent Scientific), respectively. In some experiments, a selective inverse agonist of the a5-$GABA_A$Rs, L-655,708 (50 nM; Tocris-Cookson, Ellisville, MO, USA), a GABA transporter inhibitor SKF89976A (1 mM, Tocris), or GABA (5 μM; Sigma, St Louis, MO, USA) were added to the ACSF. Synaptic plasticity was induced by repetitive stimulation at 10 Hz for 1 s, which was delivered three times at 30 s intervals. Data acquisition (filtered at 2–3 kHz and digitized at 10 kHz) was performed using a Multiclamp 700B amplifier and Clampex 10.2 software (Molecular Devices).

Data analysis

Data were analysed using Clampfit 10.2 (Molecular Devices) and Igor Pro (WaveMetrics, Lake Oswego, OR, USA). IPSC kinetics was analysed from average traces (typically, 10–15 traces) obtained after removal of 'failures' and traces contaminated with spontaneous events. The latency was measured as the time interval between the centre of the stimulation artifact and the beginning of the IPSC. IPSC amplitudes were measured at the peak of the waveform and, for group data, were normalized to the mean amplitude obtained during the baseline period (first 5 min). The rise time was defined as the duration of 20–80% of the IPSC peak amplitude. The decay phase of the IPSCs was fitted with a single exponential. Charge transfer via eIPSCs was calculated from the integral of their averaged waveforms. sIPSCs were analysed using the search events algorithm of Clampfit 10.2 and were also fitted with a single exponential. Only those events that were not contaminated by ambiguous deflections at their rising or decaying phases, and decayed back to the baseline, were selected for analysis. Typically, 200 events per cell were chosen for analysis. The paired-pulse ratio (PPR) of eIPSCs was calculated as the ratio between the mean peak amplitude of the second response and the mean peak amplitude of the first response. The coefficient of variation (CV) of eIPSCs was calculated as the ratio between the standard deviation of current amplitude and the mean current amplitude. For the analysis of the holding current and synaptic noise, the mean baseline current (defined as the mean of the peak-to-peak amplitudes of individual points) and the root-mean-square (RMS) of noise were sampled during 50 ms epochs, every 500 ms; epochs that contained spontaneous synaptic events were discarded. Subsequently, the average data of 10 s samples with uncontaminated baseline current were analysed immediately before and 10 min after bath application of L-655,708 or GABA. To compare data obtained from a group of neurons, the mean of the holding current and the RMS of noise before and after drug application were averaged. Data are presented as means ± SEM and were analysed using a Student's paired and unpaired t test, Pearson correlation or the Kolmogorov–Smirnov test, as appropriate.

Anatomical reconstruction

Neurons were filled with biocytin (0.15–0.2%; Sigma) during recordings. Slices with recorded cells were fixed overnight with 4% paraformaldehyde at 4°C. To reveal biocytin, slices were treated with hydrogen peroxide (0.3%) for 30 min, rinsed in Tris-buffered saline (TBS; pH 7.4, $t = 25$°C), permeabilized with 3% Triton X-100 (Glickfeld & Scanziani, 2006) for 1 h, and incubated overnight at 4°C with a streptavidin-conjugated Alexa-546 (dilution, 1:200; Jackson Immunoresearch, West Grove, PA, USA) in TBS containing 1% normal goat serum and 0.5% bovine serum albumin. The following day, sections were rinsed with TBS and mounted in Dako fluorescence medium (Dako Canada Inc., Missisauga, ON, Canada). Confocal images of biocytin-filled INs were obtained using a Leica TCS SP5 imaging system coupled to a 543 nm HeNe laser. Confocal Z stacks (1 μm step) containing different parts of INs were merged using Neurolucida 8.26.2 (MBF Bioscience, Williston, VT, USA) and selected cells were reconstructed.

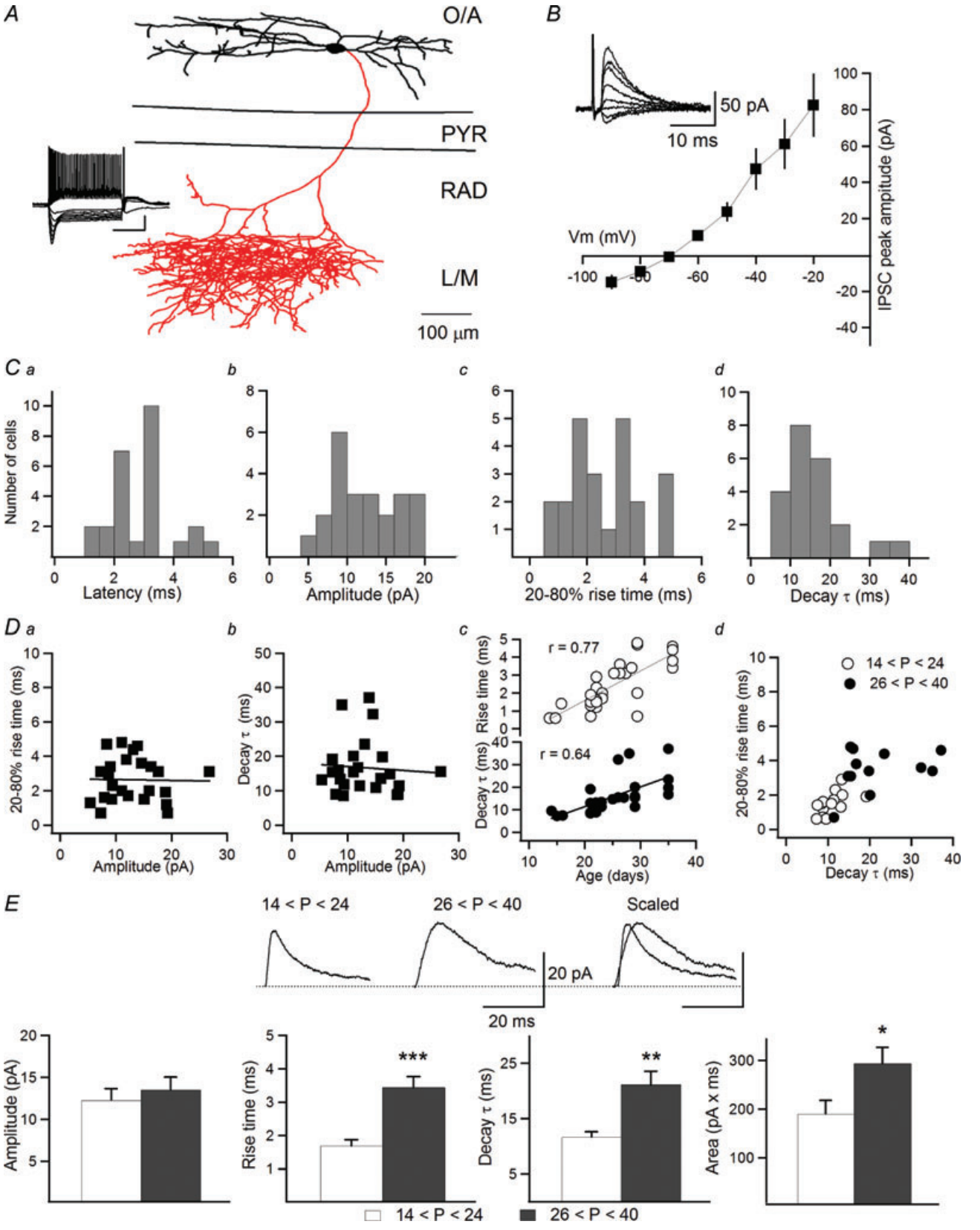

Figure 1. Age-dependent modifications in inhibitory transmission onto O-LM INs
A, neurolucida reconstruction of an O-LM IN filled with biocytin. Dendrites are shown in black and the axon is shown in red; the inset shows firing pattern and membrane properties of the reconstructed IN. Note the significant

Results

Kinetic properties of IPSCs in O-LM INs

A major problem in the study of cortical inhibitory INs is the immense heterogeneity of INs, which arises from their complex anatomical, neurochemical and functional organization (Freund & Buzsaki, 1996; Ascoli *et al.* 2008; Klausberger & Somogyi, 2008). In addition, distinct types of INs demonstrate cell-type- and even synapse-specific properties of transmission (Tóth & McBain, 1998; Lapointe *et al.* 2004; Glickfeld & Scanziani, 2006), which render the rigorous identification of INs a necessary step. Thus, we focused our study on CA1 INs with a soma and horizontally oriented dendrites that were located in the O/A, and with an axon projecting to the stratum lacunosum moleculare, i.e. the O-LM cells (Lacaille *et al.* 1987; Blasco-Ibáñez & Freund, 1995; Sik *et al.* 1995). Among 293 INs recorded in the O/A, 193 neurons were labelled successfully with biocytin and were reconstructed anatomically. Of these cells, 146 neurons were identified as O-LM INs based on a combination of anatomical criteria and electrophysiological properties (prominent I_h current, rebound spike); these cells were included in the present study (Fig. 1*A*).

Initially, we examined the properties of monosynaptic IPSCs evoked in O-LM INs by minimal stimulation of the stratum pyramidale–stratum radiatum border in the presence of 50 μM DL-AP5 and 10 μM NBQX. As the symmetrical Cl^- concentration used frequently in electrophysiological experiments affects the time course of IPSCs (Houston *et al.* 2009), we recorded IPSCs using an internal solution with low Cl^-, which is typically found in mature neurons. Under these conditions, eIPSCs in O-LM INs had a reversal potential of -71.9 ± 1.2 mV ($n = 24$; Fig. 1*B*). Furthermore, eIPSCs recorded at -40 mV had a latency that is typical of monosynaptic responses (2.97 ± 0.22 ms; $n = 24$; Fig. 1*Ca*) and a relatively small amplitude (12.93 ± 1.02 pA, $n = 24$; Fig. 1*Cb*). The rise time and the decay time constant showed significant variability among different cells (rise time: 2.64 ± 0.26 ms (0.7–4.8 ms); decay τ: 16.73 ± 1.64 ms (8.5–37.1 ms); $n = 24$; Fig. 1*Cc* and *d*). This variability was not due to a difference in dendritic attenuation of eIPSCs arising at proximal *vs.* distal synapses, as no relationship was found between the eIPSC amplitude and the rise time or the decay time constant (Fig. 1*Da* and *b*). Unexpectedly, both the rise time and the decay time constant increased significantly with animal age (Fig. 1*Dc*; $P < 0.001$; Pearson correlation). As a result, eIPSCs recorded in the O-LM INs of slices obtained from juvenile animals (P14–24) demonstrated significantly faster kinetics than those recorded in slices from adult animals (P26–40) (Fig. 1*Dd*). The rise time (juvenile: 1.69 ± 0.18 ms, $n = 11$; adult: 3.44 ± 0.32 ms, $n = 13$; $P < 0.001$), the decay time constant (juvenile: 11.66 ± 0.95 ms, $n = 11$; adult: 21.01 ± 2.34 ms, $n = 13$; $P < 0.01$) and, accordingly, the area under the curve of eIPSCs (juvenile: 189.82 ± 27.5 pA $\times$ ms, $n = 11$; adult: 292.73 ± 32.6 pA $\times$ ms, $n = 13$; $P < 0.05$) were significantly different between the two age groups (Fig. 1*E*). Thus, a considerable slowing in eIPSC kinetics followed by an overall increase in the total charge transfer was observed during synapse maturation.

We also looked for a potential age-dependent modification in synaptic kinetics by recording sIPSCs at +14 mV (which in our recording conditions corresponded to the reversal potential for EPSC). Similar to our findings regarding eIPSCs, both the rise time (juvenile: 2.18 ± 0.18 ms, $n = 10$; adult: 2.63 ± 0.15 ms, $n = 8$; $P < 0.0001$, Kolmogorov–Smirnov test) and the decay time constant (juvenile: 9.41 ± 0.6 ms, $n = 10$; adult: 10.82 ± 0.6 ms, $n = 8$; $P < 0.0001$, Kolmogorov–Smirnov test) of sIPSCs were significantly different between the two age groups (Fig. 2*B*). However, relatively small differences in sIPSC kinetics were observed compared to those of eIPSCs, suggesting that the age-dependent modifications may occur in a subset of synapses.

Age-dependent contribution of the a5-$GABA_A$R subunit to phasic inhibition of O-LM INs

Age-dependent slowing in eIPSC kinetics could originate from changes in IN morphology (e.g. dendritic growth and formation of distant synapses in INs of adult animals), age-dependent changes in GABA release and/or uptake or developmental modifications in $GABA_A$R subunit composition. These possibilities were tested. First, the total dendritic length of O-LM INs reconstructed

hyperpolarization-activated current (I_h) and a rebound depolarization followed by an action potential. O/A, stratum oriens/alveus; PYR, stratum pyramidale; RAD, stratum radiatum; L/M, lacunosum moleculare. Scale bars: 20 mV and 300 ms. *B*, *I–V* relationship of eIPSCs recorded in O-LM INs showing a reversal potential of -71.9 ± 1.2 mV; the inset demonstrates the sample traces of eIPSCs recorded at different levels of membrane potential. *C*, latency, amplitude, rise time and decay time constant distributions of eIPSCs from all cells ($n = 24$). *D*, scatter plots of rise time (*Da*) and decay time constant (*Db*) *vs.* eIPSC amplitude. *Dc*, plot of rise time and decay time constant of eIPSCs *vs.* animal age. *Dd*, plot of rise time *vs.* decay time constant of eIPSCs recorded in slices from juvenile ($n = 11$) and adult ($n = 13$) animals. *E*, sample traces (top) and summary bar graphs (bottom) of eIPSC properties in juvenile and adult animals, showing significant slowing down of eIPSCs and corresponding increase in the total charge transfer in older animals. $^*P < 0.05$; $^{**}P < 0.01$; $^{***}P < 0.001$. Error bars throughout represent the SEM.

anatomically was not significantly different between the two age groups (juvenile: $5468 \pm 419\ \mu$m, $n = 6$; adult: $6055 \pm 708\ \mu$m, $n = 6$; $P > 0.05$), suggesting that changes in the IN morphology could not contribute to IPSC kinetic modifications. Second, the eIPSC amplitude (juvenile: 12.28 ± 1.38 pA, $n = 11$; adult: 13.48 ± 1.53 pA, $n = 13$; $P > 0.05$), the PPR (juvenile: 0.71 ± 0.06, $n = 11$; adult: 0.61 ± 0.05, $n = 13$; $P > 0.05$) and the CV (juvenile: 0.2 ± 0.04, $n = 11$; adult: 0.21 ± 0.09, $n = 13$; $P > 0.05$) were not significantly different between the two age groups, indicating that the age-dependent changes in GABA release also could not account for the observed phenomenon. To examine next whether the IPSC slowing could result from a decrease in GABA uptake in adult animals, we analysed the eIPSC kinetics in the presence of the GABA transporter inhibitor SKF89976A (1 mM). However, inhibiting GABA uptake increased the rise time and the decay time constant of eIPSCs by a similar degree in INs of both juvenile and adult animals (juvenile rise: $189.3 \pm 43.5\%$ of the control, adult rise: $217.5 \pm 72\%$ of the control; juvenile decay: $177.5 \pm 66\%$ of the control, adult decay: $187 \pm 48\%$ of the control; $n = 10$, $P > 0.05$), suggesting that changes in GABA uptake also could not contribute to the age-dependent IPSC slowing.

Age-dependent modifications in the eIPSC kinetics in O-LM INs can be associated with a synapse-specific modification in $GABA_AR$ subunit composition during maturation. The a5-$GABA_ARs$ subunit is expressed abundantly in the CA1 region of the adult hippocampus

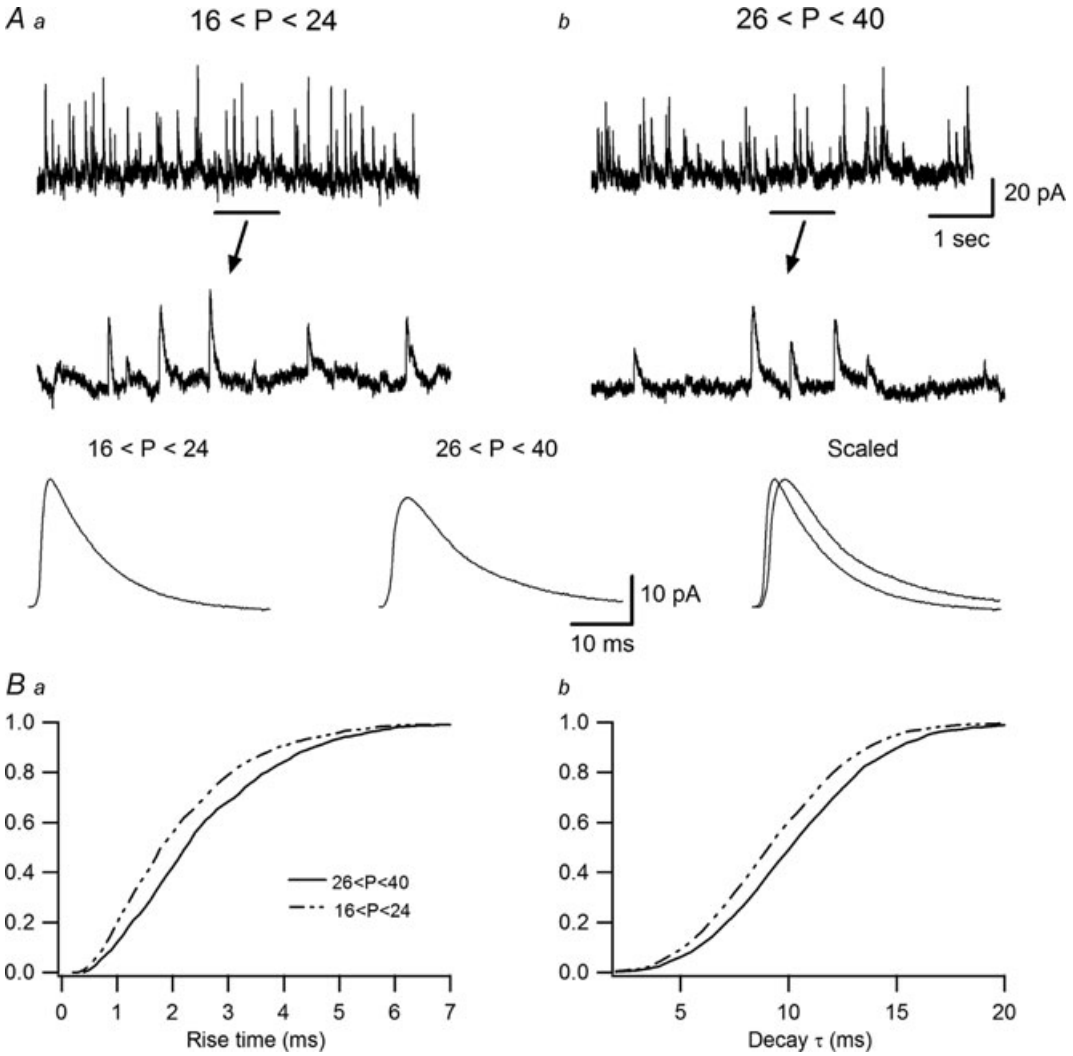

Figure 2. Comparison of kinetics of spontaneous IPSCs in O-LM INs of juvenile and adult animals
A, recording sample (top) with enlarged view showing individual events (middle) and average responses (bottom) of sIPSCs in juvenile (*Aa*; $n = 10$) and adult (*Ab*; $n = 8$) animals, demonstrating a slower kinetics in mature INs. *B*, cumulative probability plots of the rise time (*Ba*) and decay time constant (*Bb*), showing significant differences in the sIPSC kinetics between the two age groups. Kolmogorov–Smirnov statistics indicate the presence of significant *P* values ($P < 0.0001$) for both parameters.

(Wisden *et al.* 1992; Sperk *et al.* 1997), reaching its peak at P30 (Yu *et al.* 2006). Given that, in addition to tonic inhibition, this subunit is implicated in a synapse-specific manner in the generation of slow phasic inhibitory responses (Prenosil *et al.* 2006; Ali & Thomson, 2008; Zarnowska *et al.* 2009), it is possible that its age-dependent expression at inhibitory synapses onto O-LM INs is involved in the slowing of the eIPSC. To test this possibility, we first compared the effect of bath application of the a5-$GABA_A$Rs subunit inverse agonist L-655,708 (50 nM) on eIPSCs in the two age groups (Fig. 3). At low concentrations, this compound is almost 50-fold more selective for α5-containing $GABA_A$Rs compared with heteromeric complexes containing α1, α2, α3 or α6 subunits (Quirk *et al.* 1996; Casula *et al.* 2001). Our data showed that L-655,708 had no effect on IPSC amplitude in O-LM INs in slices from juvenile animals ($95.7 \pm 9.2\%$ of the control, $n = 6$, $P > 0.05$; Fig. 3*A* and *D*), but decreased the amplitude of IPSCs significantly in slices from adult mice ($72.4 \pm 3.8\%$ of the control, $n = 5$, $P < 0.05$; Fig. 3*B* and *D*). This gradually developing decrease in IPSC amplitude was not a result of IPSC run-down, as IPSC amplitude was stable in age-matched control experiments of the same duration (Fig. 3*C*).

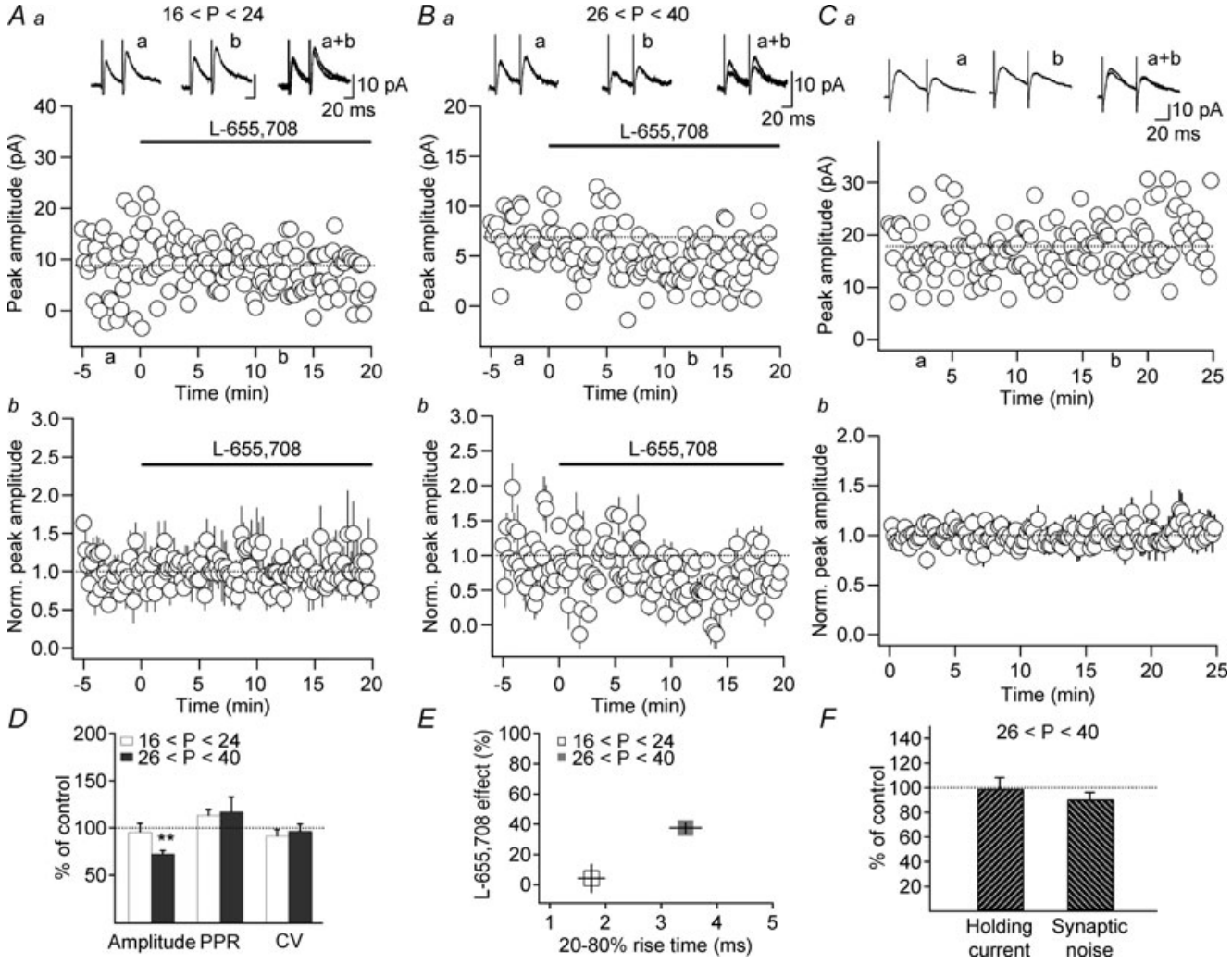

Figure 3. The a5-$GABA_A$Rs subunit mediates slow IPSCs in adult animals
A–C, scatter plots of eIPSC amplitude over time from representative recordings (*Aa*, *Ba*) and summary plots of normalized eIPSC amplitude (*Ab*, *Bb*, *Cb*; normalized to the first 5 min of recordings) obtained from juvenile (*A*; $n = 4$) and adult (*B* and *C*; $n = 5$) animals and illustrating the effect of the a5-$GABA_A$Rs inverse agonist L-655,708 (*B*, 50 nM) and the stability of eIPSC amplitude during control recording (*C*). The traces at the top are the averages of 30 consecutive IPSCs obtained at the time indicated. *D*, summary bar graphs showing changes in eIPSC amplitude, PPR and CV following L-655,708 application in the two age groups. Note a significant decrease in eIPSC amplitude after L-655,708 application in adult animals. *E*, the effect of L-655,708 correlated well with eIPSC rise time and was more prominent in cases of slower eIPSCs recorded in adult animals. *F*, bar graphs showing that L-655,708 had no effect on the holding current and synaptic noise in O-LM INs recorded in slices from adult animals. $^*P < 0.05$.

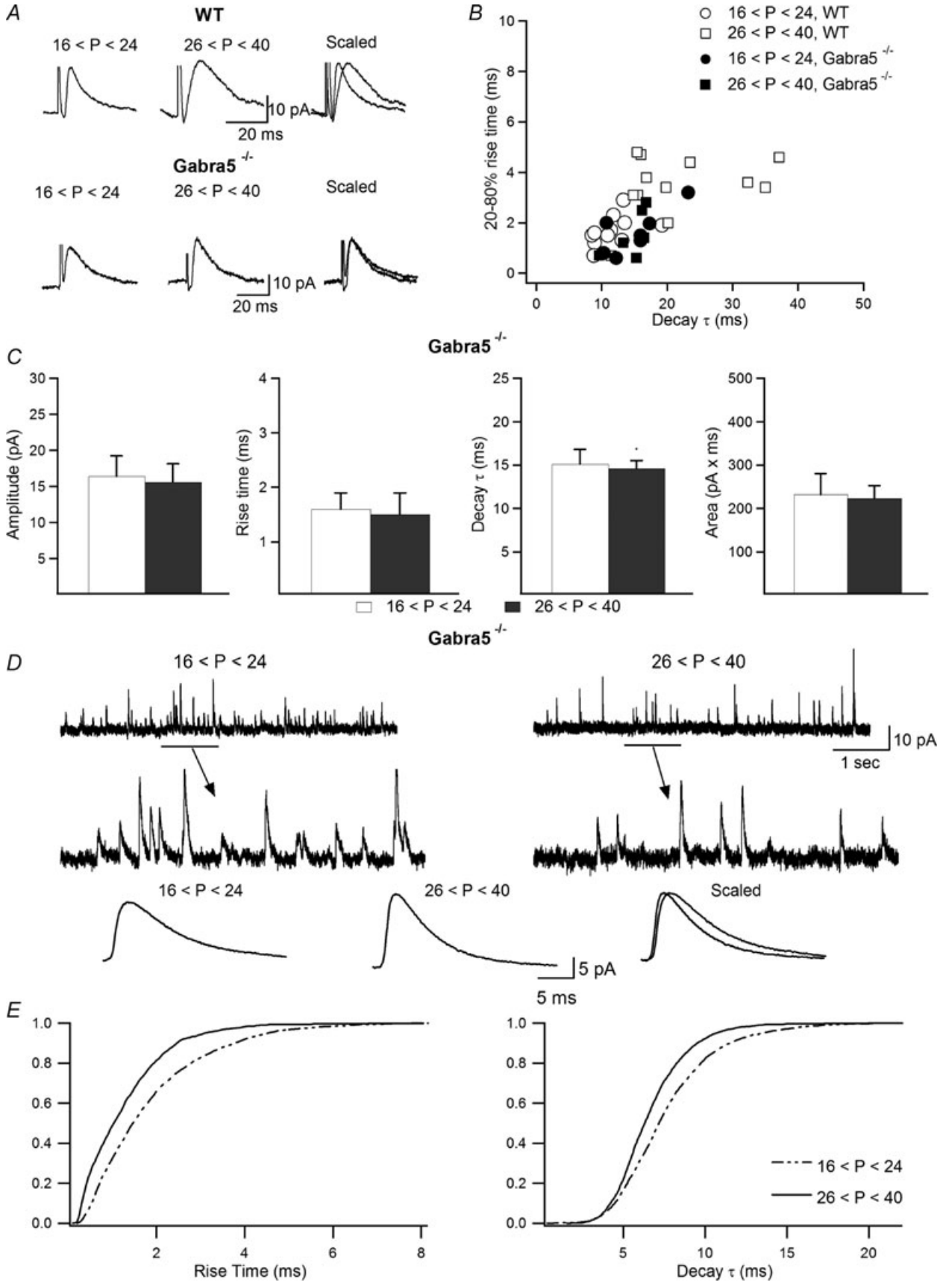

Moreover, L-655,708 had no effect on IPSC amplitude in O-LM INs in slices from adult a5-GABA$_A$Rs knockout (Gabra5$^{-/-}$) mice (97.3 ± 8.7% of the control, $n = 5$, $P > 0.05$), validating its selectivity for the a5-GABA$_A$R subunit at the concentration used. Interestingly, in adult animals, the response kinetics became significantly faster in the presence of the compound (control rise: 3.4 ± 0.3 ms, L-655,708 rise: 2.6 ± 0.3 ms; control decay: 21.3 ± 3.7 ms, L-655,708 decay: 12.7 ± 1.4 ms; $n = 6$; $P < 0.05$). Furthermore, its effect was not associated with significant changes in the PPR (juvenile: 113.4 ± 6.2% of the control, $n = 6$, $P > 0.05$; adult: 117.2 ± 15.6% of the control, $n = 5$, $P > 0.05$) or the CV (juvenile: 91.5 ± 6.8% of the control, $n = 6$, $P > 0.05$; adult: 96.5 ± 7.5% of the control, $n = 5$, $P > 0.05$), suggesting that it acts at a postsynaptic site (Fig. 3*D*). Interestingly, the effect of L-655,708 correlated well with the rise time of eIPSCs, in such a way that slower rise times were associated with a more pronounced effect of the compound (juvenile rise time: 1.75 ± 0.24 ms, L-655,708 effect: 4.3 ± 9.2%, $n = 6$; adult rise time: 3.44 ± 0.28 ms, L-655,708 effect: 37.6 ± 3.8%, $n = 5$; Fig. 3*E*). To determine whether, as observed in pyramidal cells (Caraiscos *et al.* 2004; Glykys & Mody, 2006; Prenosil *et al.* 2006), the a5-GABA$_A$R subunit is also implicated in tonic inhibition in O-LM INs, we next examined the effect of L-655,708 on the holding current and the synaptic noise in adult INs. However, our data showed that neither of the parameters was affected by the application of the compound (holding current: 99.0 ± 9.0% of the control; synaptic noise: 90.6 ± 5.6% of the control; $n = 5$; $P > 0.05$, Fig. 3*F*), which indicates the absence of tonic inhibition involving the a5-GABA$_A$R subunit in INs, under basal conditions. All above-mentioned experiments were performed in standard ACSF, at near-physiological temperature (30–33°C). However, in such conditions, tonic inhibition can be essentially obscured by the highly efficient GABA uptake system (Mody & Pearce, 2004; Glykys & Mody, 2007). To verify whether tonic inhibition can be rescued in O-LM INs by increasing the ambient concentration of GABA, GABA (5 μM) was added to the ACSF, and fluctuations in the holding current and synaptic noise were examined. However, even increased ambient GABA did not produce any significant changes in either of these parameters ($n = 4$; data not shown), suggesting that O-LM INs may not exhibit tonic inhibition. Together, these data point to the synapse-specific targeting of a5-GABA$_A$Rs subunit in O-LM INs, which occurs later during postnatal maturation.

If age-dependent synaptic expression of the a5-GABA$_A$R subunit contributes to slowing of eIPSCs in O-LM INs during maturation, then removal of the subunit should eliminate the developmental modifications in eIPSC kinetics. Accordingly, we found no differences in the rise time (juvenile: 1.6 ± 0.3 ms, $n = 7$; adult: 1.5 ± 0.4 ms, $n = 6$; $P > 0.05$), decay time constant (juvenile: 15.1 ± 1.7 ms, $n = 7$; adult: 14.6 ± 1.1 ms, $n = 6$; $P > 0.05$) or area under the curve of eIPSCs (juvenile: 232.1 ± 48.2 pA × ms, $n = 7$; adult: 223.2 ± 28.8 pA × ms, $n = 6$; $P > 0.05$) between the two age groups in Gabra5$^{-/-}$ mice (Fig. 4*A*–*C*). Moreover, in contrast to wild-type animals, sIPSCs recorded in INs from adult Gabra5$^{-/-}$ mice showed significantly faster rise time (juvenile: 1.9 ± 0.3 ms, $n = 7$; adult: 1.31 ± 0.1 ms, $n = 6$; $P < 0.0001$, Kolmogorov–Smirnov test) and decay time constant (juvenile: 7.76 ± 0.53 ms, $n = 7$; adult: 6.7 ± 0.22, $n = 6$; $P < 0.0001$, Kolmogorov–Smirnov test; Fig. 4*D* and *E*), indicating that compensatory changes may occur in a5-GABA$_A$R knockout animals leading to a preferential expression of other GABA$_A$R subunits with faster kinetics. Taken together, these results show that developmentally regulated synaptic incorporation of the a5-GABA$_A$R subunit is responsible for the slowing of eIPSC kinetics in O-LM INs during postnatal maturation.

Long-term plasticity at inhibitory synapses on O-LM INs

At least two distinct forms of long-term plasticity have been documented at excitatory synapses onto O-LM INs (Perez *et al.* 2001; Lamsa *et al.* 2007); however, the existence of any form of long-lasting modification at inhibitory synapses onto these cells remains unknown. Our data show that, regardless of the induction protocol (10 Hz *vs.* 100 Hz stimulation), synapses that form onto O-LM INs by local GABAergic projections do not

Figure 4. Loss of slow IPSCs in Gabra5$^{-/-}$ mice
A, representative examples of eIPSCs recorded in the two age groups in wild-type and Gabra5$^{-/-}$ animals. *B*, scatter plot of the rise time *vs.* decay time constant of eIPSCs obtained in slices from Gabra5$^{-/-}$ mice compared to wild-type animals, showing a fast kinetics of events in both age groups in slices from Gabra5$^{-/-}$ animals. *C*, summary bar graphs of eIPSC properties in juvenile and adult Gabra5$^{-/-}$ animals, showing a loss of age-dependent eIPSC modifications in older animals in the absence of the a5-GABA$_A$Rs subunit. Error bars throughout represent the SEM. *D*, sample trace (top) with enlarged view showing individual events (middle) and average traces (bottom) of sIPSCs recorded in INs from juvenile and adult Gabra5$^{-/-}$ mice, demonstrating faster sIPSC kinetics in mature INs. *E*, cumulative probability plots of the rise time (left) and decay time constant (right), showing significantly faster sIPSC kinetics in INs from adult animals ($n = 6$; $P < 0.0001$, Kolmogorov–Smirnov test).

exhibit long-term plasticity in slices from juvenile animals (Chamberland *et al.* 2010). Therefore, next we tested the hypothesis that age-dependent synaptic remodelling involving the a5-$GABA_AR$ subunit can be associated with an emergence of long-term plasticity at inhibitory synapses onto these cells. The comparison of the effect of 10 Hz stimulation (which mimics the endogenous theta rhythm in the hippocampus) on the eIPSC amplitude between the two age groups revealed that the eIPSC amplitude remained unchanged 20 min after stimulation in O-LM INs of slices from juvenile animals (104.4 ± 3.1% of the control, $n = 4$; $P > 0.05$, Fig. 5*Aa* and *Ba*). A short-term depression followed by an increase in the PPR and CV was observed in 5 out of 6 cells from this group (5 min after

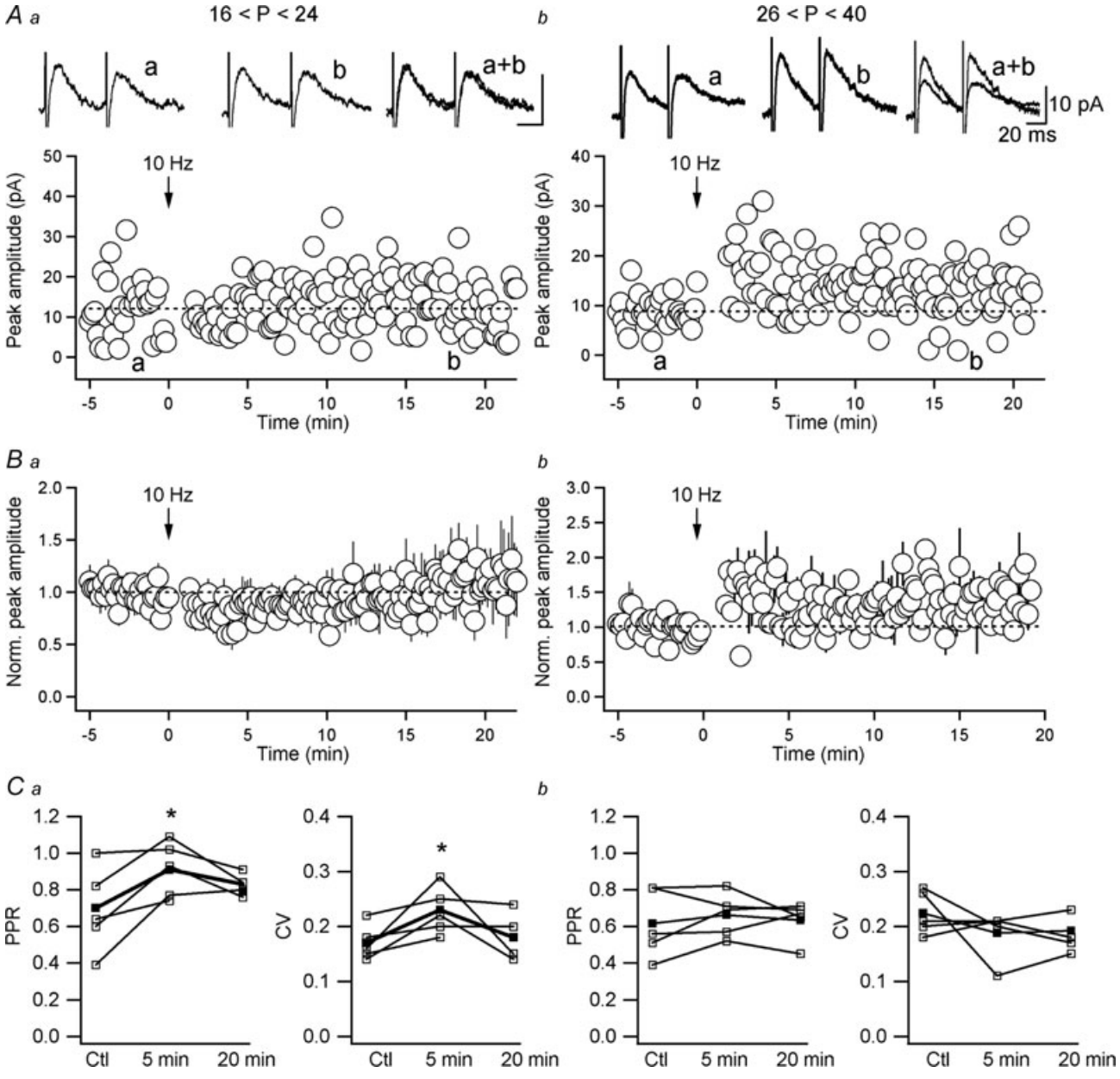

Figure 5. Developmental expression of LTP at inhibitory synapses onto O-LM INs
A and *B*, representative recordings (*Aa*, *Ab*) and normalized group data (*Ba*, *Bb*) of eIPSC amplitude obtained from INs of juvenile (*A*; $n = 4$) and adult (*B*; $n = 5$) mice, showing short-term depression of eIPSCs induced by 10 Hz stimulation in INs of juvenile animals and long-term potentiation (LTP) of eIPSCs in mature INs. The traces at the top are average eIPSCs (average of 30 sweeps) in control (a), 20 min after tetanization (b), as well as their superimposition. *C*, summary graphs showing changes in the eIPSC PPR and CV induced by 10 Hz stimulation in juvenile (*Ca*) and adult (*Cb*) animals. Note that LTP of eIPSCs in O-LM INs was not associated with changes in PPR or CV (*Cb*), indicating a postsynaptic locus for its expression.

induction IPSC amplitude: 75.4 ± 2.2% of the control, PPR: 140.6 ± 16.7% of the control, CV: 136.6 ± 13.9% of the control, $n = 5$; $P < 0.05$, Fig. 5*Ba* and *Ca*), pointing to a presynaptic locus of its expression. In contrast, long-term potentiation (LTP) of eIPSCs was revealed in O-LM INs of adult mice (141.7 ± 6.3% of the control, $n = 5$; $P < 0.05$, Fig. 5*Ab* and *Bb*). LTP was expressed postsynaptically, as no change was observed in the PPR (102.9 ± 5.5% of the control, $n = 5$, $P > 0.05$, Fig. 5*Cb*) or CV (85.7 ± 6.3% of the control, $n = 5$; $P > 0.05$, Fig. 5*Cb*). These results suggest that the maturation of inhibitory synapses onto O-LM INs is followed by an overall increase in the inhibition of these cells via slowing of their IPSC kinetics and emergence of LTP in response to theta-like activity.

As the a5-$GABA_A$R subunit was, up to this point, responsible for the age-dependent remodelling of inhibitory synapses onto O-LM INs, we next assessed its implication in the LTP of IPSCs uncovered in INs in slices from adult animals (Fig. 6). Our data showed that LTP was blocked in the presence of L-655,708 (eIPSC amplitude: 112.7 ± 14.3% of the control; $n = 6$; $P > 0.05$, Fig. 6*Aa* and *Ba*), as well as in Gabra5$^{-/-}$ mice (eIPSC amplitude: 86.4 ± 10.3% of the control; $n = 5$; $P > 0.05$, Fig. 6*Ab* and *Bb*). Taken together, these data indicate that, in addition to its role in slowing down the IPSC kinetics, the a5-$GABA_A$R subunit, which is expressed later during development at inhibitory synapses onto O-LM INs, is directly associated with an emergence of LTP at these

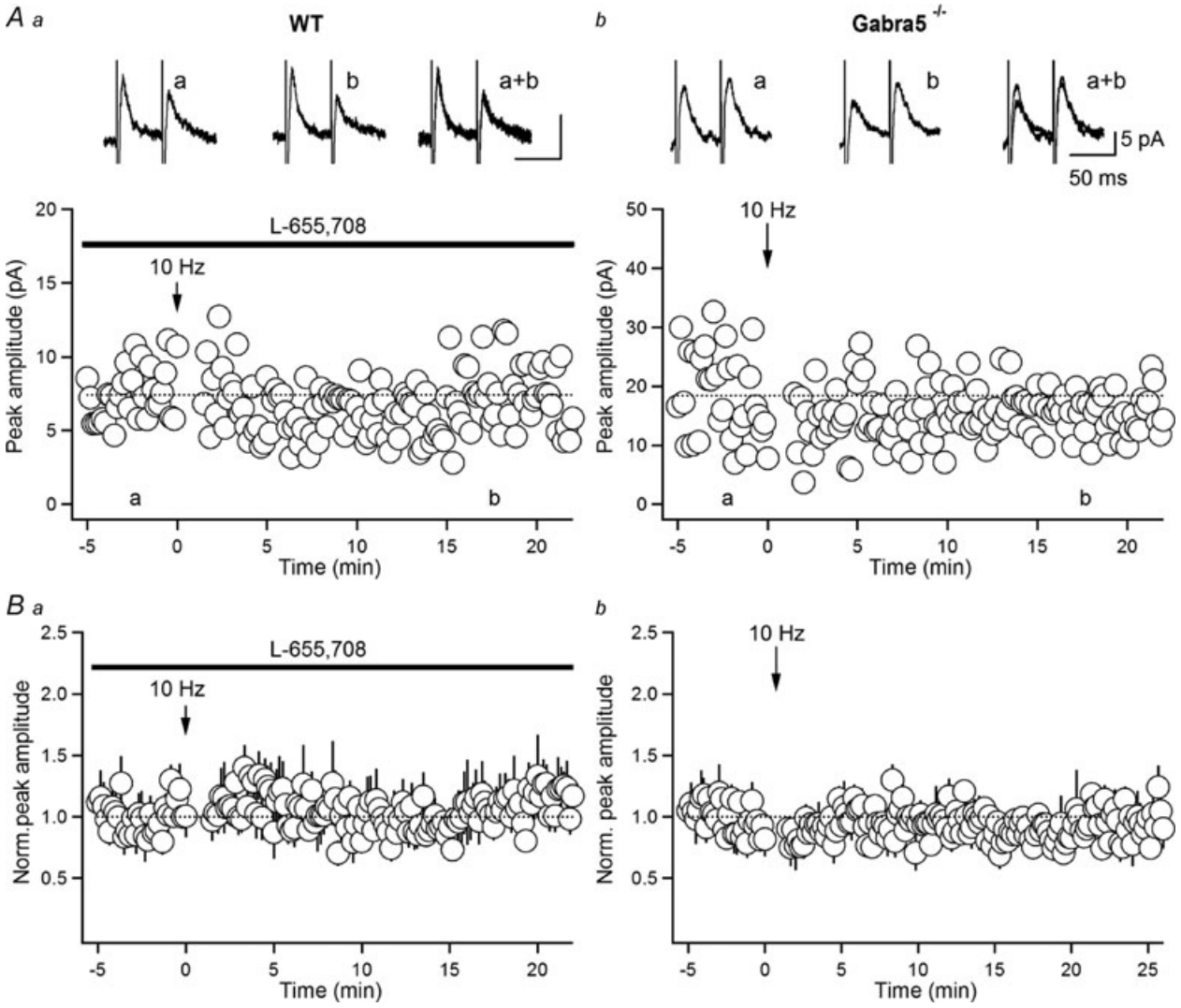

Figure 6. The a5-$GABA_A$Rs subunit is involved in LTP at inhibitory synapses onto O-LM INs
A and *B*, scatter plots of eIPSC amplitude over time from representative recordings (*Aa*, *Ab*) and summary plots of normalized IPSC amplitude (*Ba*, *Bb*; normalized to the first 5 min of recordings) obtained in INs from adult mice in the presence of the a5-$GABA_A$Rs inverse agonist L-655,708 (*Aa* and *Ba*; $n = 6$) and in Gabra5$^{-/-}$ adult animals (*Ab* and *Bb*; $n = 6$), showing the absence of LTP of eIPSCs in both conditions. Traces at the top are the averages of 30 consecutive eIPSCs obtained at the time indicated.

synapses and, therefore, represents a primary mechanism for the strengthening of the local inhibition of O-LM INs in the mature hippocampus.

Functional consequences of inhibitory synapse remodelling for IN excitability

Finally, we investigated whether the maturation of inhibitory synapses, followed by synaptic incorporation of the a5-$GABA_A$R subunit and slowing of the IPSC kinetics, would have any consequences for O-LM IN excitability. INs were recorded in current-clamp mode and were tonically depolarized for 2 s to allow a continuous spiking with an average frequency of 10 Hz, during which an inhibitory postsynaptic potential (IPSP) (in the presence of DL-AP5 and NBQX) was evoked (Fig. 7*A*). Consistent with our findings, IPSPs evoked in O-LM INs in slices from adult animals exhibited significantly slower rise time (juvenile: 2.3 ± 0.2 ms, $n = 6$; adult: 4.7 ± 0.5 ms, $n = 5$; $P < 0.001$) and decay time constant (juvenile: 15.0 ± 2.8 ms, $n = 6$; adult: 32.6 ± 7.2 ms, $n = 5$; $P < 0.05$), whereas their amplitudes remained similar in the two age groups (juvenile: -2.0 ± 0.6 mV; $n = 6$; adult: -2.1 ± 0.6 mV, $n = 5$; $P > 0.05$; Fig. 7*B* and *D*). Furthermore, in both age groups the generation of IPSPs resulted in the immediate cessation of action potentials (Fig. 7*A*–*C*) and the duration of the silence episodes was much longer in INs of adult animals (Fig. 7*C*). Accordingly, the latency for the first spike following the silence episodes was significantly prolonged in INs of adult animals compared with those of juvenile mice (juvenile: 79 ± 8.7 ms, $n = 6$; adult: 147.8 ± 17.2 ms, $n = 5$; $P < 0.01$; Fig. 7*D* and *E*). The longer spike firing inhibition episodes found in mature INs were not caused by different firing rate and/or adaptation as the average firing frequency was similar in both age groups and it remained unchanged before (juvenile: 11.5 ± 1.1 Hz, $n = 6$; adult: 11.1 ± 1.2 Hz, $n = 5$, $P > 0.05$) and after (juvenile: 10.1 ± 0.5 Hz, $n = 6$; adult: 10.6 ± 0.9 Hz, $n = 5$, $P > 0.05$) the generation of the IPSP (Fig. 7*C*). Importantly, eIPSP amplitude (-1.68 ± 0.3 mV), rise time (2.61 ± 0.2 ms), decay time constant (11.2 ± 1.2 ms) and, accordingly, the spike latency (82.7 ± 13.7 ms) in interneurons of adult Gabra5$^{-/-}$ mice were not significantly different from those in interneurons of juvenile WT animals ($n = 7$, $P > 0.05$; Fig 7*D* and *E*). Taken together, our findings strongly indicate that age-dependent strengthening of O-LM IN inhibition due to synaptic incorporation of the a5-$GABA_A$Rs subunit is likely to have a profound effect on IN excitability and firing behaviour.

Discussion

Here, we investigated the properties and plasticity of GABAergic synapses onto O-LM INs, a main source of dendritic feedback inhibition to pyramidal neurons that controls the integration of the perforant path. One of our major findings is that inhibitory synapses onto these cells undergo significant remodelling during postnatal maturation. First, the kinetics of eIPSCs exhibited a marked slowing down in INs of adult animals, with a net increase in the total charge transfer of ∼50%. These kinetic modifications of synaptic inhibitory currents were attributed to the age-dependent synaptic incorporation of the a5-$GABA_A$R subunit. Furthermore, the a5-$GABA_A$R subunit, expressed later during development at IN inhibitory synapses, was responsible for the delayed emergence of LTP at these synapses. Importantly, our findings show that the a5-$GABA_A$R-mediated prolongation of synaptic inhibition had a profound effect on IN firing, which was significantly delayed following the activation of inhibitory synapses in INs of adult animals. Thus, the age-dependent remodelling of GABAergic synapses via synaptic incorporation of the a5-$GABA_A$R subunit, followed by the overall strengthening of local inhibition of O-LM cells, represents a new mechanism of inhibitory synapse maturation and is likely to have important functional consequences on the operation of the hippocampal feedback inhibitory circuitry.

The maturation of cortical inhibitory circuits plays an important role in the tuning of neuronal connections during critical periods of development. As evidenced by multiple anatomical and functional studies, the maturation of inhibitory circuits, followed by the postnatal increase in the number of inhibitory synapses and in the levels of GABA-synthesizing enzymes as well as by complex modifications in the $GABA_A$ response properties (Luhmann & Prince, 1991; Agmon *et al.* 1996; Dunning *et al.* 1999; Morales *et al.* 2002), is completed only by postnatal week 5. Age-dependent alterations in the kinetics of IPSCs associated with changes in $GABA_A$ receptor subunit composition have been reported in cerebellar granule cells (Tia *et al.* 1996) and in cortical (Dunning *et al.* 1999; Bosman *et al.* 2005; Kobayashi *et al.* 2008) and thalamic laterodorsal neurons (Okada *et al.* 2000). As a rule, a progressively faster IPSC kinetics, associated with an increase in the expression of the a1-$GABA_A$R or a6-$GABA_A$R subunits (Tia *et al.* 1996; Dunning *et al.* 1999; Bosman *et al.* 2005) and with the concomitant decrease in the level of a2-$GABA_A$Rs (Dunning *et al.* 1999), has been reported in neurons of the mature brain. The first case of the age-dependent slowing of inhibitory synapses has been demonstrated in hippocampal CA1 pyramidal cells, where it was associated with a differential age-dependent recruitment of some classes of INs (Banks *et al.* 2002). Our study also reports the age-dependent slowing down of inhibitory transmission at GABAergic synapses but the mechanism involves modifications in the $GABA_A$ receptor subunit composition. Importantly, this phenomenon was uncovered at inhibitory synapses

formed onto inhibitory INs. As very little is known currently about the developmental regulation of inhibition within largely interconnected inhibitory circuits, our findings begin to reveal the interneuron-specific rules of maturation of inhibitory synapses. Accordingly, we found a major role for the a5-$GABA_AR$ subunit in the age-dependent slowing down of IPSCs. Several unique features set the a5-$GABA_AR$ apart from others. First,

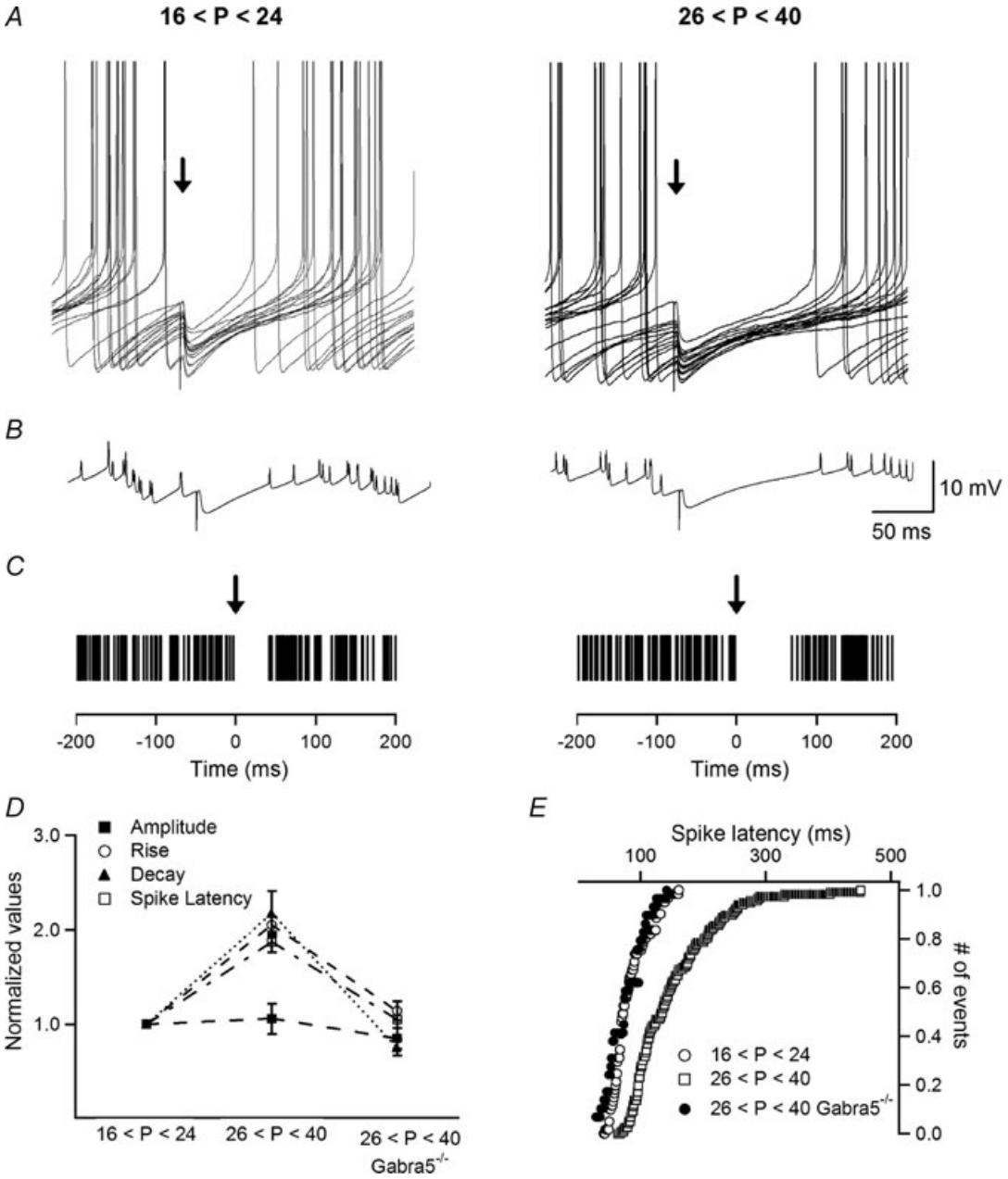

Figure 7. Age-dependent strengthening of inhibition decreased IN firing
A, representative examples of current-clamp recordings of IN firing during which IPSPs (indicated by an arrow) were evoked in juvenile and adult animals. *B*, averages of the traces shown in *A* demonstrating a significant slowing down in IPSP kinetics and a prolongation of the firing silence episodes in mature INs. *C*, summary raster plots of the distribution of action potentials before and after IPSP generation, demonstrating the age-dependent prolongation of the firing silence episodes, together with unchanged firing frequency. *D*, summary plot showing the age-dependent differences (normalized to the values obtained in the juvenile group) in IPSP amplitude, rise time, decay time constant and spike latency between the two age groups in WT and in adult Gabra5$^{-/-}$ mice. *E*, cumulative distribution of first spike latencies after the generation of IPSPs in the two age groups of WT animals and in adult Gabra5$^{-/-}$ mice. Note a significant prolongation in the spike latency in mature INs in WT mice ($n = 5$; $P < 0.01$) but not in Gabra5$^{-/-}$ mice.

it is expressed primarily in the hippocampus, reaching ∼25% of all $GABA_A$Rs (Wisden *et al.* 1992; Sur *et al.* 1998; Pirker *et al.* 2000). So far, its expression has been reported only in pyramidal cells whereas our data provide evidence for this subunit expression in inhibitory interneurons. Interestingly, expression of the a5-$GABA_A$R peaks at postnatal day 30 (Yu *et al.* 2006). Second, the subunit can be located at both synaptic and extrasynaptic sites (Brunig *et al.* 2002; Serwanski *et al.* 2006) and, therefore, it can be involved in tonic and phasic inhibition (Collinson *et al.* 2002; Caraiscos *et al.* 2004; Scimemi *et al.* 2005; Glykys & Mody, 2006; Prenosil *et al.* 2006; Ali & Thomson, 2008; Zarnowska *et al.* 2009). The implication of a5-$GABA_A$Rs in phasic inhibition is likely to be synapse specific (Ali & Thomson, 2008; Zarnowska *et al.* 2009), pointing to the synapse-specific trafficking and anchoring mechanisms necessary for its differential expression (Loebrich *et al.* 2006). Third, when expressed synaptically, the a5-$GABA_A$R subunit mediates responses that are kinetically slow (Prenosil *et al.* 2006; Ali & Thomson, 2008; Zarnowska *et al.* 2009). The latter may be associated with the slower desensitization rate reported for this subunit compared with the a1-$GABA_A$R-containing receptors in a recombinant system (Caraiscos *et al.* 2004). Finally, the a5-$GABA_A$R subunit is involved in the regulation of hippocampal network excitability (Scimemi *et al.* 2005; Glykys & Mody, 2006) and hippocampus-dependent learning, so that its deletion or pharmacological blockade in animals improves their overall performance during learning tasks (Chambers *et al.* 2002; Collinson *et al.* 2002).

Consistent with previous findings of the possible synaptic expression of a5-$GABA_A$Rs, our data showed that this receptor subunit can be involved in synaptic inhibition in hippocampal inhibitory INs in a synapse-specific manner. Current evidence indicates that inhibitory synapses onto O-LM INs are formed by at least two inputs: a septal GABAergic projection and a local inhibitory input originating from the type III interneuron-selective INs (ISIs) (Acsády *et al.* 1996; Gulyas *et al.* 1996; Chamberland *et al.* 2010), although other projections from oriens–oriens INs have also been suggested (Fukuda & Kosaka, 2000). These inputs innervate different domains of O-LM cells (perisomatic *vs.* dendritic) via synapses with distinct kinetic properties (Chamberland *et al.* 2010). By stimulating in the stratum pyramidale adjacent to stratum radiatum, we could preferentially activate the ISI projection, which innervates the dendrites of O-LM INs. This would explain profound modifications in kinetics of eIPSCs compared to those of sIPSCs. Age-dependent synaptic incorporation of the a5-$GABA_A$R subunit was not reported previously, although a possible developmental upregulation of this subunit is evidenced by the apparent increase in its density during postnatal maturation and ageing (Yu *et al.* 2006). The fact that the a5-$GABA_A$R subunit populates synaptic and extrasynaptic sites and contributes functionally to distinct forms of inhibition in principal neurons suggests a highly versatile subunit scaffolding machinery that is able to form and maintain the functional receptors all across the neuronal surface. However, the mechanisms that control the synapse-specific incorporation of a5-$GABA_A$Rs in INs remain unclear. Interestingly, the actin-binding ERM-family protein radixin plays a critical role in the anchoring and localization of a5-$GABA_A$Rs (Loebrich *et al.* 2006). However, the synapse-specific expression of radixin, which would explain the preferential targeting of a5-$GABA_A$Rs, has not been demonstrated.

Our finding of a postsynaptic form of LTP, which required intact a5-$GABA_A$Rs, points to a novel form of plasticity at inhibitory synapses that may operate in mature inhibitory networks. The developmental factors that may initiate specific synaptic incorporation of a5-$GABA_A$Rs in INs and, more importantly, the mechanisms that may control the emergence of long-term synaptic plasticity involving this subunit remain unknown. Activity-dependent regulation of $GABA_A$Rs by protein phosphorylation, which affects the receptor ion channel properties or open probability as well as receptor trafficking and recruitment, are well-established phenomena that occur at inhibitory synapses (Moss *et al.* 1995; McDonald *et al.* 1998; Nusser *et al.* 1999; Brunig *et al.* 2002; Houston *et al.* 2008; Bannai *et al.* 2009). Remarkably, LTP induction at inhibitory synapses onto INs may not require the same mechanisms as in pyramidal cells (e.g. $GABA_B$ or metabotropic glutamate receptors), pointing to distinct mechanisms of plasticity induction at synapses on INs (Patenaude *et al.* 2005). Here, no attempt was made to identify the molecular mechanisms required for the induction and expression of LTP. However, as no age-dependent changes in the overall activity of INs (firing pattern and frequency) were observed in the present study, other mechanisms may operate specifically at IN inhibitory synapses, driving synaptic incorporation of the a5-$GABA_A$R subunit during maturation. Glial cells, which support different aspects of synapse development (Pfrieger, 2002), are a possible source of such signals. Interestingly, the maturation of inhibitory synapses observed here parallels the morphological and functional maturation of astrocytes (Kressin *et al.* 1995; Bushong *et al.* 2004). As these cells release several regulatory molecules and factors, it would be logical to expect their potential contribution to the age-dependent inhibitory synaptic modification (Pfrieger, 2002).

The final question addressed in this study was whether the age-dependent remodelling of inhibitory synapses had any functional consequences for IN activity. Our findings suggest that inhibitory synapse maturation, followed by a significant reinforcement of local inhibitory input to O-LM cells, controls the overall excitability and firing behaviour of INs. The effect of IPSP prolongation

was dramatic, as it increased the duration of silence episodes in mature INs by almost 100%. Importantly, this finding raises new questions regarding the functional consequences of the efficient IN inhibition for its dendritic integration and spike generation (Martina *et al.* 2000), synaptic plasticity (Lamsa *et al.* 2007) and brain-state-dependent implication of O-LM INs in network activity (Klausberger *et al.* 2003). How would increased inhibition affect dendritic Ca^{2+} signalling in O-LM cells: would it facilitate Ca^{2+} signals via Ca^{2+}-permeable AMPA receptors compared with other Ca^{2+} sources (Topolnik *et al.* 2005) and, as a result, the induction of the anti-Hebbian form of LTP at IN excitatory synapses (Lamsa *et al.* 2007)? How would increased inhibition affect the dendritic initiation and propagation of Na^+ (Martina *et al.* 2000) and/or Ca^{2+} spikes (Topolnik *et al.* 2005) and overall dendritic electrogenesis? Would the prolongation of silence episodes evoked by the activation of inhibitory synapses in mature O-LM INs have an effect on the IN recruitment during hippocampal rhythmic activity, leading, for instance, to a delayed recruitment at particular phases of theta oscillations or to longer silence periods during sharp-wave-associated ripples (Klausberger *et al.* 2003)? Finally, how would these age-dependent modifications in the activity of O-LM INs affect the integration of the perforant path by pyramidal neurons and the local circuit dialogue? Clearly, the next step is to define the molecular details underlying the maturation of the inhibitory synapse in O-LM INs and its consequences for the operation of INs and local circuitry.

References

Acsády L, Görcs TJ & Freund T (1996). Different populations of vasoactive intestinal polypeptide-immunoreactive interneurons are specialized to control pyramidal cells or interneurons in the hippocampus. *Neuroscience* **73**, 317–334.

Agmon A, Hollrigel G & O'Dowd DK (1996). Functional GABAergic synaptic connection in neonatal mouse barrel cortex. *J Neurosci* **15**, 4685–4695.

Ali AB (2007). Presynaptic inhibition of GABAA receptor-mediated unitary IPSPs by cannabinoid receptors at synapses between CCK-positive interneurons in rat hippocampus. *J Neurophysiol* **98**, 861–869.

Ali AB & Thomson AM (2008). Synaptic α5 subunit-containing GABAA receptors mediate IPSPs elicited by dendrite-preferring cells in rat neocortex. *Cereb Cortex* **18**, 1260–1271.

Ascoli GA, Alonso-Nanclares L, Anderson SA, Barrionuevo G, Benavides-Piccione R, Burkhalter A *et al.* (2008). Petilla terminology: nomenclature of features of GABAergic interneurons of the cerebral cortex. *Nat Rev Neurosci* **9**, 557–568.

Banks MI, Hardie J & Pearce R (2002). Development of GABAA receptor-mediated inhibitory postsynaptic currents in hippocampus. *J Neurophysiol* **88**, 3097–3107.

Bannai H, Lévi S, Schweizer C, Inoue T, Launey T, Racine V *et al.* (2009). Activity-dependent tuning of inhibitory neurotransmission based on GABAAR diffusion dynamics. *Neuron* **62**, 670–682.

Bartos M, Vida I, Frotscher M, Geiger J & Jonas P (2001). Rapid signaling at inhibitory synapses in a dentate gyrus interneuron network. *J Neurosci* **21**, 2687–2698.

Blasco-Ibáñez JM & Freund T (1995). Synaptic input of horizontal interneurons in stratum oriens of the hippocampal CA1 subfield: structural basis of feed-back activation. *Eur J Neurosci* **17**, 2170–2180.

Bosman LW, Heinen K, Spijker S & Brussaard AB (2005). Mice lacking the major adult GABAA receptor subtype have normal number of synapses, but retain juvenile IPSC kinetics until adulthood. *J Neurophysiol* **94**, 338–346.

Brunig I, Scotti E, Sidler C & Fritschy JM (2002). Intact sorting, targeting, and clustering of γ-aminobutyric acid A receptor subtypes in hippocampal neurons *in vitro*. *J Comp Neurol* **443**, 43–55.

Buhl EH, Cobb SR, Halasy K & Somogyi P (1995). Properties of unitary IPSPs evoked by anatomically identified basket cells in the rat hippocampus. *Eur J Neurosci* **7**, 1989–2004.

Bushong EA, Martone ME & Ellisman MH (2004). Maturation of astrocyte morphology and the establishment of astrocyte domains during postnatal hippocampal development. *Int J Dev Neurosci* **22**, 73–86.

Caraiscos VB, Elliott EM, You-Ten KE, Cheng VY, Belelli D, Newell JG *et al.* (2004). Tonic inhibition in mouse hippocampal CA1 pyramidal neurons is mediated by α5 subunit-containing γ-aminobutyric acid type A receptors. *Proc Natl Acad Sci U S A* **101**, 3662–3667.

Casula MA, Bromidge F, Pillai G, Wingrove P, Martin K, Maubach K *et al.* (2001). Identification of amino acid residues responsible for the α5 subunit binding selectivity of L-655,708, a benzodiazepine binding site ligand at the $GABA_A$ receptor. *J Neurochem* **77**, 445–451.

Chamberland S, Salesse C, Topolnik D & Topolnik L (2010). Synapse-specific inhibitory control of hippocampal feedback inhibitory circuit. *Front Cell Neurosci* **4**, 130.

Chambers MS, Atack JR, Bromidge FA, Broughton HB, Cook S, Dawson GR *et al.* (2002). 6,7-Dihydro-2-benzothiophen-4(5H)-ones: a novel class of GABA-A α5 receptor inverse agonists. *J Med Chem* **45**, 1176–1179.

Cobb SR, Halasy K, Vida I, Nyiri G, Tamás G, Buhl EH & Somogyi P (1997). Synaptic effects of identified interneurons innervating both interneurons and pyramidal cells in the rat hippocampus. *Neuroscience* **79**, 629–648.

Collinson N, Kuenzi FM, Jarolimek W, Maubach KA, Cothliff R, Sur C *et al.* (2002). Enhanced learning and memory and altered GABAergic synaptic transmission in mice lacking the α5 subunit of the GABAA receptor. *J Neurosci* **22**, 5572–5580.

Dunning DD, Hoover CL, Soltesz I, Smith MA & O'Dowd DK (1999). $GABA_A$ receptor-mediated miniature postsynaptic currents and α-subunit expression in developing cortical neurons. *J Neurophysiol* **82**, 3286–3297.

Fox JG (2007). *The Mouse in Biomedical Research*, pp. 1600. Academic Press.

Freund TF & Buzsaki G (1996). Interneurons of the hippocampus. *Hippocampus* **6**, 347–470.

Fritschy JM & Mohler H (1995). GABAA-receptor heterogeneity in the adult rat brain: differential regional and cellular distribution of seven major subunits. *J Comp Neurol* **359**, 154–194.

Fukuda T & Kosaka T (2000). Gap junctions linking the dendritic network of GABAergic interneurons in the hippocampus. *J Neurosci* **20**, 1519–1528.

Glickfeld LL & Scanziani M (2006). Distinct timing in the activity of cannabinoid-sensitive and cannabinoid-insensitive basket cells. *Nat Neurosci* **9**, 807–815.

Glykys J & Mody I (2006). Hippocampal network hyperactivity after selective reduction of tonic inhibition in $GABA_A$ receptor α5 subunit-deficient mice. *J Neurophysiol* **95**, 2796–2807.

Glykys J & Mody I (2007). Activation of GABAA receptors: views from outside the synaptic cleft. *Neuron* **56**, 763–770.

Gulyás A, Hájos N & Freund T (1996). Interneurons containing calretinin are specialized to control other interneurons in the rat hippocampus. *J Neurosci* **16**, 3397–3411.

Hájos N & Mody I (1997). Synaptic communication among hippocampal interneurons: properties of spontaneous IPSCs in morphologically identified cells. *J Neurosci* **17**, 8427–8442.

Houston CM, Bright DP, Sivilotti LG, Beato M & Smart TG (2009). Intracellular chloride ions regulate the time course of GABA-mediated inhibitory synaptic transmission. *J Neurosci* **29**, 10416–10423.

Houston CM, He Q & Smart T (2008). CaMKII phosphorylation of the GABAA receptor: receptor subtype- and synapse-specific modulation. *J Physiol* **87**, 2115–2125.

Karson MA, Tang AH, Milner T & Alger BE (2009). Synaptic cross talk between perisomatic-targeting interneuron classes expressing cholecystokinin and parvalbumin in hippocampus. *J Neurosci* **29**, 4140–4154.

Klausberger T, Magill PJ, Marton LF, Roberts JD, Cobden PM, Buzsaki G & Somogyi P (2003). Brain-state- and cell-type-specific firing of hippocampal interneurons *in vivo*. *Nature* **421**, 844–848.

Klausberger T & Somogyi P (2008). Neuronal diversity and temporal dynamics: the unity of hippocampal circuit operations. *Science* **321**, 53–57.

Kobayashi M, Hamada T, Kogo M, Yanagawa Y, Obata K & Kang Y (2008). Developmental profile of GABAA-mediated synaptic transmission in pyramidal cells of the somatosensory cortex. *Eur J Neurosci* **28**, 849–861.

Kressin K, Kuprijanova E, Jabs R, Seifert G & Steinhäuser C (1995). Developmental regulation of Na^+ and K^+ conductances in glial cells of mouse hippocampal brain slices. *Glia* **15**, 173–187.

Lacaille JC, Mueller AL, Kunkel DD & Schwartzkroin PA (1987). Local circuit interactions between oriens/alveus interneurons and CA1 pyramidal cells in hippocampal slices: electrophysiology and morphology. *J Neurosci* **7**, 1979–1993.

Lamsa KP, Heeroma JH, Somogyi P, Rusakov DA & Kullmann DM (2007). Anti-Hebbian long-term potentiation in the hippocampal feedback inhibitory circuit. *Science* **315**, 1262–1266.

Lapointe V, Morin F, Ratte S, Croce A, Conquet F & Lacaille JC (2004). Synapse-specific mGluR1-dependent long-term potentiation in interneurones regulates mouse hippocampal inhibition. *J Physiol* **15**, 125–135.

Loebrich S, Bähring R, Katsuno T, Tsukita S & Kneussel M (2006). Activated radixin is essential for GABAA receptor α5 subunit anchoring at the actin cytoskeleton. *EMBO J* **25**, 987–999.

Luhmann HJ & Prince DA (1991). Postnatal maturation of the GABAergic system in rat neocortex. *J Neurophysiol* **65**, 247–263.

Maccaferri G & Lacaille JC (2003). Interneuron diversity series: hippocampal interneuron classifications–making things as simple as possible, not simpler. *Trends Neurosci* **26**, 564–571.

Martina M, Vida I & Jonas P (2000). Distal initiation and active propagation of action potentials in interneuron dendrites. *Science* **287**, 295–300.

McBain CJ & Fisahn A (2001). Interneurons unbound. *Nat Rev Neurosci* **2**, 11–23.

McDonald BJ, Amato A, Connolly CN, Benke D, Moss SJ & Smart TG (1998). Adjacent phosphorylation sites on GABAA receptor β subunits determine regulation by cAMP-dependent protein kinase. *Nat Neurosci* **1**, 23–28.

Mody I & Pearce RA (2004). Diversity of inhibitory neurotransmission through $GABA_A$ receptors. *Trends Neurosci* **27**, 569–575.

Morales B, Choi SY & Kirkwood A (2002). Dark rearing alters the development of GABAergic transmission in visual cortex. *J Neurosci* **22**, 8084–8090.

Moss SJ, Gorrie GH, Amato A & Smart TG (1995). Modulation of GABAA receptors by tyrosine phosphorylation. *Nature* **377**, 344–348.

Nusser Z, Sieghart W & Mody I (1999). Differential regulation of synaptic GABAA receptors by cAMP-dependent protein kinase in mouse cerebellar and olfactory bulb neurones. *J Physiol* **521**, 421–435.

Nusser Z, Sieghart W & Somogyi P (1998). Segregation of different GABAA receptors to synaptic and extrasynaptic membranes of cerebellar granule cells. *J Neurosci* **18**, 1693–1703.

Okada M, Onodera K, Van Renterghem C, Sieghart W & Takahashi T (2000). Functional correlation of $GABA_A$ receptor α subunits expression with the properties of IPSCs in the developing thalamus. *J Neurosci* **20**, 2202–2208.

Patenaude C, Massicotte G & Lacaille JC (2005). Cell-type specific GABA synaptic transmission and activity-dependent plasticity in rat hippocampal stratum radiatum interneurons. *Eur J Neurosci* **22**, 179–188.

Patenaude C, Nurse S & Lacaille JC (2001). Sensitivity of synaptic $GABA_A$ receptors to allosteric modulators in hippocampal oriens-alveus interneurons. *Synapse* **41**, 29–39.

Perez Y, Morin F & Lacaille JC (2001). A hebbian form of long-term potentiation dependent on mGluR1 a in hippocampal inhibitory interneurons. *Proc Natl Acad Sci U S A* **98**, 9401–9406.

Pfrieger FW (2002). Role of glia in synapse development. *Cur Opinion Neurobiol* **12**, 486–490.

Pirker S, Schwarzer C, Wieselthaler A, Sieghart W & Sperk G (2000). $GABA_A$ receptors: immunocytochemical distribution of 13 subunits in the adult rat brain. *Neuroscience* **101**, 815–850.

Prenosil GA, Schneider Gasser EM, Rudolph U, Keist R, Fritschy JM & Vogt KE (2006). Specific subtypes of GABAA receptors mediate phasic and tonic forms of inhibition in hippocampal pyramidal neurons. *J Neurophysiol* **96**, 846–857.

Quirk K, Blurton P, Fletcher S, Leeson P, Tang F, Mellilo D *et al*. (1996). [3 H]L-655,708, a novel ligand selective for the benzodiazepine site of GABAA receptors which contain the α5 subunit. *Neuropharmacology* **35**, 1331–1335.

Ribak CE (1978). Aspinous and sparsely-spinous stellate neurons in the visual cortex of rats contain glutamic acid decarboxylase. *J Neurocytol* **7**, 461–478.

Scimemi A, Semyanov A, Sperk G, Kullmann DM & Walker MC (2005). Multiple and plastic receptors mediate tonic GABAA receptor currents in the hippocampus. *J Neurosci* **25**, 10016–10024.

Serwanski DR, Miralles C, Christie S, Mehta A, Li X & De Blas AL (2006). Synaptic and nonsynaptic localization of GABAA receptors containing the α5 subunit in the rat brain. *J Comp Neurol* **499**, 458–470.

Sik A, Penttonen M, Ylinen A & Buzsaki G (1995). Hippocampal CA1 interneurons: an in vivo intracellular labeling study. *J Neurosci* **15**, 6651–6665.

Soltesz I (2006). *Diversity in the Neuronal Machine. Order and Variability in Interneuronal Microcircuits*. Oxford University Press, Oxford.

Sperk G, Schwarzer C, Tsunashima K, Fuchs K & Sieghart W (1997). $GABA_A$ receptor subunits in the rat hippocampus I: immunocytochemical distribution of 13 subunits. *Neuroscience* **80**, 987–1000.

Sur C, Quirk K, Dewar D, Atack J & McKernan R (1998). Rat and human hippocampal α5 subunit-containing γ-aminobutyric acid A receptors have α5 β3 γ2 pharmacological characteristics. *Mol Pharmacol* **54**, 928–933.

Tia S, Wang JF, Kotchabhakdi N & Vicini S (1996). Developmental changes of inhibitory synaptic currents in cerebellar granule neurons: role of $GABA_A$ receptor α6 subunit. *J Neurosci* **16**, 3630–3640.

Topolnik L, Congar P & Lacaille JC (2005). Differential regulation of mGluR- and AMPAR-mediated dendritic Ca^{2+} signals by pre- and postsynaptic activity in hippocampal interneurons. *J Neurosci* **25**, 990–1001.

Tóth K & McBain CJ (1998). Afferent-specific innervation of two distinct AMPA receptor subtypes on single hippocampal interneurons. *Nat Neurosci* **1**, 572–578.

Wisden W, Laurie DJ, Monyer H & Seeburg PH (1992). The distribution of 13 GABAA receptor subunit mRNAs in the rat brain. I. Telencephalon, diencephalon, mesencephalon. *J Neurosci* **12**, 1040–1062.

Yu ZY, Wang W, Fritschy JM, Witte OW & Redecker C (2006). Changes in neocortical and hippocampal GABAA receptor subunit distribution during brain maturation and aging. *Brain Res* **1099**, 73–81.

Zarnowska ED, Keist R, Rudolph U & Pearce RA (2009). GABAA receptor α5 subunits contribute to GABAA slow synaptic inhibition in mouse hippocampus. *J Neurophysiol* **101**, 1179–1191.

Author contributions

C.S., C.L.M. and S.C. collected and analysed the data and took part in the manuscript preparation. L.T. designed the experiments, analysed the data and wrote the manuscript. All authors approved the final version.

Acknowledgements

We thank Dr Istvan Mody for the generous gift of the Gabra5 KO mouse line and for comments that greatly improved the manuscript, Karen Vandal (laboratory of Dr Yves De Koninck) for help with Gabra5 KO colony, Dimitry Topolnik for excellent technical assistance and cell reconstruction, Tatyana Pokidchenko and Benoit Aubé for assistance in some experiments. This work was supported by the Canadian Institutes of Health Research, the Natural Sciences and Engineering Research Council of Canada (NSERC Discovery Grant), and the Savoy Foundation. L.T. is the recipient of a University Faculty Award from NSERC. S.C. was supported by a fellowship from the Fonds de la Recherche en Santé du Québec.